

# Phase Equilibrium in the Y-Fe-O System at 1000°C

Kenzo Kitayama\*, Miyuki Takano, Kozo Eitaki, and Akihiro Hoshina

(Received October 29, 2004)

Phase equilibrium was established in the Y-Fe-O system at 1000°C with an oxygen partial pressure ranging from  $-\log(P_{O_2}/\text{atm}) = 0$  to 16.15, allowing construction of a phase diagram of the  $Y_2O_3$ -Fe- $Fe_2O_3$  system at 1000°C.  $Y_2O_3$ , Fe, "FeO",  $Fe_3O_4$ ,  $Fe_2O_3$ , and  $YFeO_3$  were found to be stable in the system.  $Y_3Fe_5O_{12}$  and  $YFe_2O_4$  were not found in the system. The present results were different from those of previous work at 1200°C, in which  $YFe_2O_4$  and  $Y_3Fe_5O_{12}$  were stable together with  $YFeO_3$ , and also different from those of previous work at 1100°C, in which only  $Y_3Fe_5O_{12}$  was stable together with  $YFeO_3$  as the ternary compounds.

Nonstoichiometric ranges were found in the FeO phase, with the composition of FeO represented as a function of  $\log(P_{O_2}/\text{atm})$ ,  $N_{O}/N_{Fe} = 4.635 \times 10^{-2} \log P_{O_2} + 1.747$ . Activities of components in the solid solution were calculated from the equation.

$YFeO_3$  lattice constants, prepared in air by the quenching method, were determined and compared with previous values. These were in good agreement with previous values. The Gibbs energy changes of the reaction  $1/2 Y_2O_3 + Fe + 3/4 O_2 = YFeO_3$ , appearing in the phase diagram, were calculated from the oxygen partial pressures in equilibrium, and the value obtained was compared with previous values.

Key words: Phase equilibrium, Thermogravimetry, Yttrium-iron oxide, Gibbs energy.

## INTRODUCTION

Phase relations in the Fe-O system have been reported from the standpoint of steelmaking (1,2,3). As is well known, there are three oxides, "FeO",  $Fe_3O_4$ , and  $Fe_2O_3$  in the Fe-O system. "FeO" has a cubic structure and forms a metal defect solid solution.  $Fe_3O_4$  has an inverse spinel structure and a short solid solution range of oxygen-rich composition side, and this range changes with temperature.  $Fe_2O_3$  has a stoichiometric composition and rhombohedral crystal system.

From JANAF data(4), the oxygen partial pressure in equilibrium with Fe and FeO, with FeO and  $Fe_3O_4$ , and with  $Fe_3O_4$  and  $Fe_2O_3$  were determined to be -14.91, -13.56, and -5.16 in  $\log(P_{O_2}/\text{atm})$  at 1000°C, respectively.

\* Professor, Department of Applied Chemistry and Biotechnology

The phases in the Y-Fe-O system are of important technological interest, particularly in view of their physical properties. As is well known,  $\text{YFeO}_3$  and  $\text{Y}_3\text{Fe}_5\text{O}_{12}$  (yttrium iron garnet, YIG) are stable in the Y-Fe-O system as ternary compounds. Notably, YIG has been used as a magnetic material, and  $\text{YFeO}_3$  and  $\text{Y}_3\text{Fe}_5\text{O}_{12}$  have been used in operational memory.

Recently, a new  $\text{YFe}_2\text{O}_4$  phase was found to be stable at  $1200^\circ\text{C}$  by Kimizuka and Katsura (5), and it has a hexagonal crystal system with  $a = 6.090 \text{ \AA}$  and  $c = 24.788 \text{ \AA}$ . Piekarczyk et al. (6) have reported the  $\text{YFe}_2\text{O}_4$  phase to be stable above  $1010^\circ\text{C}$ . According to Kato et al. (7), the crystal structure of this compound is a new type of  $\text{AB}_2\text{X}_4$ , where A and B are cations and X is an anion, and belongs to the trigonal system with the space group  $R\bar{3}m$ . The structure consists of alternate layers of  $\text{Ln}_2\text{O}_3$  and  $\text{Fe}_4\text{O}_5$ , and thus anisotropies, both in the magnetic interaction and the electrical conductivity, are expected.

The crystal structure and magnetic properties of  $\text{YFe}_2\text{O}_4$ , together with  $\text{ErFe}_2\text{O}_4$ , have been studied by Matsumoto et al. (8), and the pressure dependence of the  $\text{YFe}_2\text{O}_4$  magnetic phase transitions was found.

Solid electrolyte galvanic cell EMF was performed on the reaction  $\text{Fe} + 3/2 \text{NiO} + 1/2 \text{Y}_2\text{O}_3 = 3/2 \text{Ni} + \text{YFeO}_3$  at  $1200\sim 1400\text{K}$ , and in combination with the Gibbs energy of NiO formation obtained by Charett et al.(9), Gibbs energy of the reaction,  $\text{Fe} + 1/2 \text{Y}_2\text{O}_3 + 3/4 \text{O}_2 = \text{YFeO}_3$ , was calculated(10).

The objectives of the present study are to: (1) establish a detailed phase diagram of Y-Fe-O system at  $1000^\circ\text{C}$  as a function of oxygen partial pressure; (2) ascertain whether  $\text{YFe}_2\text{O}_4$  and  $\text{Y}_3\text{Fe}_5\text{O}_{12}$  are stable or not; that is, whether the phase diagram at  $1000^\circ\text{C}$  is different from those at  $1200^\circ\text{C}$  and  $1100^\circ\text{C}$  or not; (3) determine the thermochemical properties of reactions based on the phase diagram at  $1000^\circ\text{C}$ .

## 2. EXPERIMENTAL

Analytical grade  $\text{Y}_2\text{O}_3$  (99.9%) and  $\text{Fe}_2\text{O}_3$  (99.9%) were used as the starting materials. Both oxides were calcined at  $1000^\circ\text{C}$ . Mixtures having desired ratios of  $\text{Y}_2\text{O}_3/\text{Fe}_2\text{O}_3$  were prepared by thoroughly mixing in an agate mortar with repeated calcination during intermediate mixings. This was followed by the same procedures as described previously (11).

The desired oxygen partial pressures were obtained by using gas mixtures of  $\text{CO}_2$  and  $\text{H}_2$ , and of  $\text{CO}_2$  and  $\text{O}_2$ , and using individual gases  $\text{O}_2$  and  $\text{CO}_2$ . The actual oxygen partial pressure of the gas phases was measured by means of a solid electrolytic cell composed of  $(\text{ZrO}_2)_{0.85}(\text{CaO})_{0.15}$ (12).

The apparatus and procedures for controlling the oxygen partial pressure, keeping a constant temperature, the thermogravimetry method, and the criterion for the establishment of equilibrium were the same as described previously (11). The method of establishing equilibrium can be briefly described as follows. To ensure equilibrium, the equilibrium weight of each sample at a particular oxygen partial pressure was determined for both sides of the reaction; that is, as the oxygen partial pressure was increased from a low value and as it was decreased from a high value. The balance, furnace, and gas mixer are schematically shown in the previous report (13). The furnace was installed vertically, and a mullite tube wound with Pt-Rh(60%-40%) alloy wire served as the heating element. To ensure the desired oxygen partial pressures, an appropriate gas mixture was passed from the bottom of the furnace to the top.

The identification of phases and the determination of lattice constants were performed using of Rint 2500 Rigaku X-ray diffractometer, employing Ni-filtered  $\text{CuK}\alpha$  radiation. An external standard silicon was used to calibrate  $2\theta$ .

### 3. RESULTS AND DISCUSSIONS

#### (1) Phase equilibrium

##### 1) Fe-O system at 1000°C.

To date, three oxides are known for the Fe-O system, "FeO",  $\text{Fe}_3\text{O}_4$ , and  $\text{Fe}_2\text{O}_3$ .

In the present experiment, the Fe-O system was reinvestigated using the present apparatus and techniques at 1000°C. The results are as follows. Figure 1a shows the

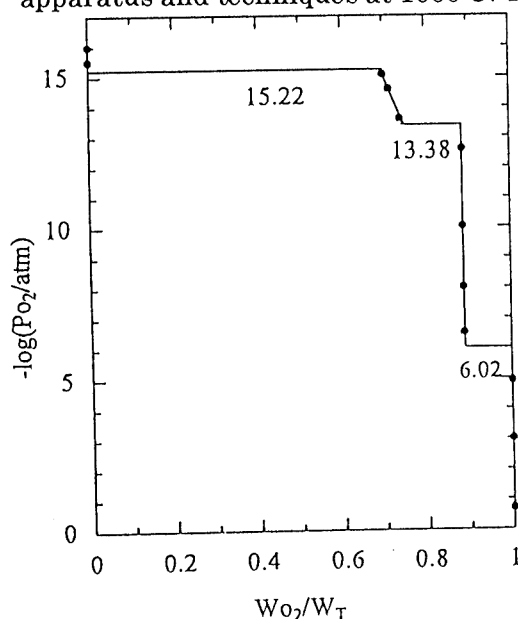


Fig. 1a. The relationship between the oxygen partial pressure,  $\log(P_{\text{O}_2}/\text{atm})$  and the weight change of samples,  $W_{\text{O}_2}/W_T$  in the Fe-O system.

oxygen partial pressure,  $-\log(P_{\text{O}_2}/\text{atm})$ , versus the weight changes,  $W_{\text{O}_2}/W_T$  of the Fe-O system. Here,  $W_{\text{O}_2}$  is the weight increase of a sample from the reference weight at  $\log(P_{\text{O}_2}/\text{atm}) = -16.15$ , at which Fe is stable, and  $W_T$  is the total weight gain from the reference state to the state at 1 atm  $\text{O}_2$ . As shown in Fig. 1a, weight breaks are found at 15.22, 13.38, and 6.02. These values correspond to the oxygen partial pressures in equilibrium of the three reactions: 1)  $\text{Fe} + 1/2 \text{O}_2 = \text{FeO}$ , 2)  $3 \text{FeO} + 1/2 \text{O}_2 = \text{Fe}_3\text{O}_4$ , and 3)  $2/3 \text{Fe}_3\text{O}_4 + 1/6 \text{O}_2 = \text{Fe}_2\text{O}_3$ , which are listed in Table 4. Figure 1b shows the relationship between the oxygen partial pressure and a

composition, the  $N_{\text{O}}/N_{\text{Fe}}$  mole fraction ratio, of the FeO solid solution. Here,  $N_{\text{O}}$  and  $N_{\text{Fe}}$  represent the mole fraction of oxygen and iron in the FeO solid solution.

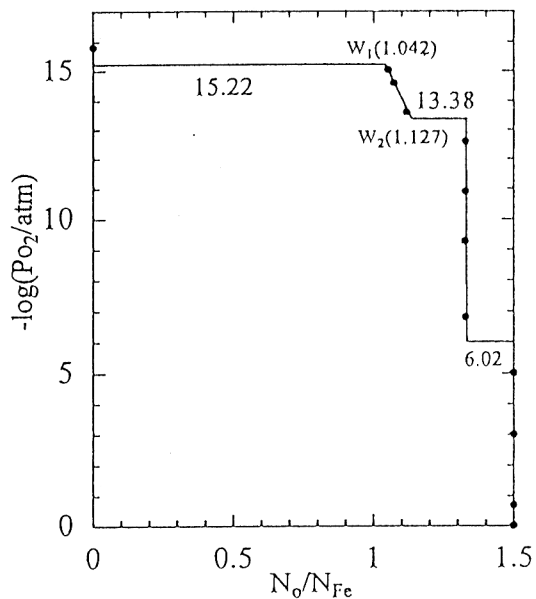


Fig. 1b. The relationship between the oxygen partial pressure,  $\log(P_{\text{O}_2}/\text{atm})$ , and the  $N_{\text{O}}/N_{\text{Fe}}$  mole fraction ratio in the Fe-O system.

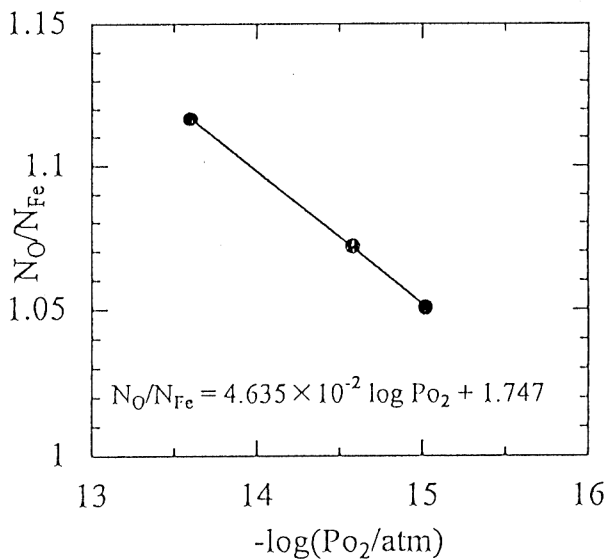


Fig. 1c. The relationship between the oxygen partial pressure,  $\log(P_{\text{O}_2}/\text{atm})$  and  $N_{\text{O}}/N_{\text{Fe}}$  in the FeO solid solution.

It is apparent that the FeO solid solution is stable in the oxygen partial pressure  $-\log P_{\text{O}_2} = 13.38 \sim 15.22$ , and that the composition of FeO in equilibrium with metallic iron is 1.042 of the  $N_{\text{O}}/N_{\text{Fe}}$  mole ratio at  $\log(P_{\text{O}_2}/\text{atm}) = -15.22$  and the composition of FeO in equilibrium with  $\text{Fe}_3\text{O}_4$  is 1.127 of the  $N_{\text{O}}/N_{\text{Fe}}$  mole ratio at  $\log(P_{\text{O}_2}/\text{atm}) = -13.38$ , respectively. The  $\log(P_{\text{O}_2}/\text{atm})$  versus the  $N_{\text{O}}/N_{\text{Fe}}$  mole ratio of FeO solid solution is shown in Fig. 1c, and is represented by an equation:  $N_{\text{O}}/N_{\text{Fe}} = 4.635 \times 10^{-2} \log P_{\text{O}_2} + 1.747$ . This equation will be used to obtain the activities of the iron and FeO components in the solid solution by the Gibbs-Duhem equation(1,14).

A slight weight increase might be observed from  $-\log(P_{\text{O}_2}/\text{atm}) = -13.38$  to 6.02 for  $\text{Fe}_3\text{O}_4$ , as is well known, although it is not evident from Fig. 1a or b because of the scale of abscissa.

## 2) $\text{Y}_2\text{O}_3\text{-Fe-Fe}_2\text{O}_3$ system.

Four samples, having  $\text{Y}_2\text{O}_3/\text{Fe}_2\text{O}_3$  molar ratios of 0.7/0.3, 0.6/0.4, 0.4/0.6, and 0.2/0.8, were prepared for thermogravimetric analysis. Figure 2 shows the oxygen partial pressure,  $-\log(P_{\text{O}_2}/\text{atm})$ , versus the weight changes,  $W_{\text{O}_2}/W_{\text{T}}$ , for three representative samples: 0.6/0.4 (Fig. 2a), 0.4/0.6 (Fig. 2b), and 0.2/0.8 (Fig. 2c). Here also,  $W_{\text{O}_2}$  is the weight increase of a sample from the reference weight at  $\log(P_{\text{O}_2}/\text{atm}) = -16.15$ , at which  $\text{Y}_2\text{O}_3$  and Fe are stable, and  $W_{\text{T}}$  is the total weight-gain from the reference state

to the state at 1 atm O<sub>2</sub>, at which Y<sub>2</sub>O<sub>3</sub> and YFeO<sub>3</sub>, and YFeO<sub>3</sub> and Fe<sub>2</sub>O<sub>3</sub> were stable, depending upon the total compositions of samples, as shown in Fig. 3. These phases

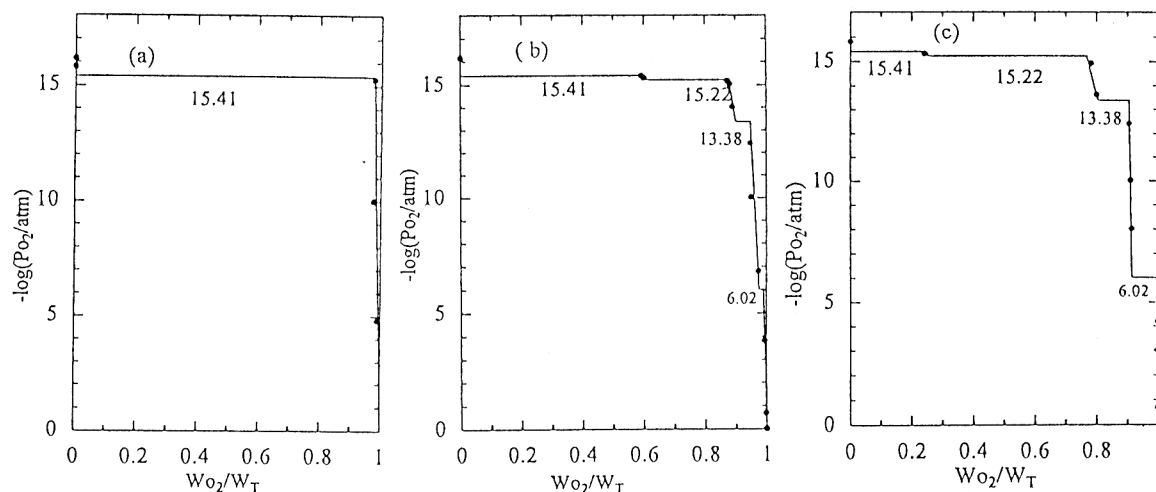


Fig. 2. The relationship between the oxygen partial pressure,  $\log(P_{O_2}/\text{atm})$ , and the weight change of the samples,  $W_{O_2}/W_T$ . (a)  $Y_2O_3/Fe_2O_3 = 0.6/0.4$ , (b)  $Y_2O_3/Fe_2O_3 = 0.4/0.6$ , and (c)  $Y_2O_3/Fe_2O_3 = 0.2/0.8$ .

were ascertained by an identification of phase. As is evident from Fig. 2, weight breaks are found at 15.41, 15.22, 13.38, and 6.02 in  $-\log(P_{O_2}/\text{atm})$ . These values correspond to the oxygen partial pressure in equilibrium with the three solid phases, Y<sub>2</sub>O<sub>3</sub> + YFeO<sub>3</sub> + Fe, YFeO<sub>3</sub> + FeO + Fe, YFeO<sub>3</sub> + FeO + Fe<sub>3</sub>O<sub>4</sub>, and YFeO<sub>3</sub> + Fe<sub>3</sub>O<sub>4</sub> + Fe<sub>2</sub>O<sub>3</sub>, respectively.

Y <sub>2</sub> O <sub>3</sub> Mol	Fe <sub>2</sub> O <sub>3</sub> ratio	$-\log P_{O_2}$ atm	Time hr	Phase
0	1.0	15.80	6.7	Fe
		14.60	7.3	FeO
		13.60	7.6	FeO
		12.50	7.4	Fe <sub>3</sub> O <sub>4</sub>
		8.50	20.9	Fe <sub>3</sub> O <sub>4</sub>
		5.00	21.0	Fe <sub>2</sub> O <sub>3</sub>
		0.68	16.0	Fe <sub>2</sub> O <sub>3</sub>
0.2	0.8	15.80	6.7	Fe + Y <sub>2</sub> O <sub>3</sub>
		15.30	6.9	Fe + YFeO <sub>3</sub>
		14.60	7.2	FeO + YFeO <sub>3</sub>
		13.60	6.8	FeO + YFeO <sub>3</sub>
		12.50	8.0	Fe <sub>3</sub> O <sub>4</sub> + YFeO <sub>3</sub>
		8.50	22.4	Fe <sub>3</sub> O <sub>4</sub> + YFeO <sub>3</sub>
		5.00	22.0	Fe <sub>2</sub> O <sub>3</sub> + YFeO <sub>3</sub>
0.4	0.6	15.80	6.7	Fe + Y <sub>2</sub> O <sub>3</sub>
		15.30	6.9	Fe + YFeO <sub>3</sub>
		14.60	7.2	FeO + YFeO <sub>3</sub>
		13.60	6.8	FeO + YFeO <sub>3</sub>
		12.50	8.0	Fe <sub>3</sub> O <sub>4</sub> + YFeO <sub>3</sub>
		8.50	22.4	Fe <sub>3</sub> O <sub>4</sub> + YFeO <sub>3</sub>
		5.00	22.0	Fe <sub>2</sub> O <sub>3</sub> + YFeO <sub>3</sub>
0.6	0.4	15.80	6.7	Fe + Y <sub>2</sub> O <sub>3</sub>
		8.50	22.4	YFeO <sub>3</sub> + Y <sub>2</sub> O <sub>3</sub>
		0.68	75.0	YFeO <sub>3</sub> + Y <sub>2</sub> O <sub>3</sub>
		0.68	75.0	YFeO <sub>3</sub> + Y <sub>2</sub> O <sub>3</sub>

Table 1 shows the results of phase identification for the Y-Fe-O system, along with the experimental conditions.

Samples of about 500mg were prepared for the phase identification by means of the quenching method. Six phases, Y<sub>2</sub>O<sub>3</sub>, Fe, FeO, Fe<sub>3</sub>O<sub>4</sub>, Fe<sub>2</sub>O<sub>3</sub>, and YFeO<sub>3</sub> were evaluated by powder X-ray analysis and were found to be stable under the experimental conditions, whereas Y<sub>3</sub>Fe<sub>5</sub>O<sub>12</sub> (YIG) and YFe<sub>2</sub>O<sub>4</sub> were not found to be stable.

From the above thermogravimetric results and phase identification, a phase diagram

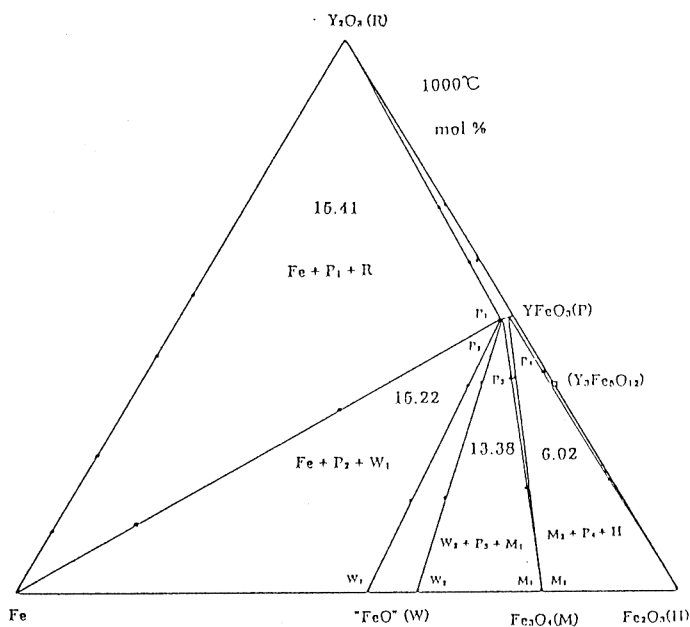


Fig. 3. Phase equilibrium in the  $Y_2O_3$ -Fe- $Fe_2O_3$  system at  $1000^\circ C$ . Numerical values indicated in the three phase regions are the oxygen partial pressures in  $-\log(P_{O_2}/atm)$  in equilibrium with the solid phases shown in each region. Abbreviations are the same as those in Table 2.

between the Y-Fe-O phase diagram of the present results and that of other author's results. The nonstoichiometry of  $YFeO_3$  was also determined, but the composition range was small. The relationship between the oxygen partial pressure and the composition  $N_O/N_{YFeO_3}$  of the  $YFeO_3$  solid solution could be represented by an equation:  $N_O/N_{YFeO_3} = -1.426 \times 10^{-4}(\log P_{O_2})^2 - 1.379 \times 10^{-4}(\log P_{O_2})$ , obtained by the least-squares method. Here,  $N_O$  and  $N_{YFeO_3}$  represent the mole fraction of oxygen and  $YFeO_3$  in the  $YFeO_3$  solid solution. This equation can be solved to show that yttrium-iron perovskite would be stoichiometric ( $YFeO_{3.00}(P)$ ) at 0 and  $YFeO_{2.97}(P_1)$  at 15.41 in terms of  $\log(P_{O_2}/atm)$ .

As described above(1-3), the  $Fe_3O_4$  phase has a small nonstoichiometry, although this is not explicitly shown in Fig. 3 because of the figure's scale.

The compositions, symbols, compounds stability ranges in oxygen partial pressures

Table 2. Compositions, Symbols, Stability Ranges of Oxygen Partial Pressures, and Activities of Components in Solid Solutions.

Component	Compositions	Symbols	$-\log(P_{O_2}/atm)$	$\log a_i$
FeO	$FeO_{1.042}$	$W_1$	15.22	0
	$FeO_{1.127}$	$W_2$	13.38	-0.0628
$YFeO_3$	$YFeO_{2.96}$	$P_1$	5.41	0
	$YFeO_{2.98}$	$P_2$	13.38	0.0280
	$YFeO_{2.99}$	$P_3$	6.02	0.0749
	$YFeO_{3.00}$	$P$	0.00	0.0788

and activities of components in the solid solutions are tabulated in Table 2. In the next section, these activities will be used in the calculation of the Gibbs energy changes of

for the  $Y_2O_3$ -Fe- $Fe_2O_3$  system was constructed. The numerical values of the three solid fields in Fig. 3 are the values of  $-\log P_{O_2}$  in equilibrium with the three solid phases described above. As described above,  $Y_3Fe_5O_{12}$  and  $YFe_2O_4$  were not stable under the present experimental conditions. Piekarczyk et al.(6) reported that "the phase diagram analysis shows for the entire temperature range investigated, from 900 to  $1250^\circ C$ , that the garnet  $Y_3Fe_5O_{12}$  can coexists with  $Fe_3O_4$  and  $Fe_2O_3$ ". This shows a striking difference

reactions.

The lattice constants of  $\text{YFeO}_3$  perovskite were determined to be orthorhombic using the  $0.6\text{Y}_2\text{O}_3/0.4\text{Fe}_2\text{O}_3$  mole ratio sample which was made at 0.68 in  $-\log P_{\text{O}_2}$ . The results are tabulated in Table 3, together with the previously reported values (15). Slight differences were found in the lattice constants.

## (2) Standard Gibbs Energy Change of Reaction

On the basis of the established phase diagram, Gibbs energy changes of reactions were determined by the equation,  $\Delta G^\circ = -RT \ln K$ . Here, R is the gas constant, T the absolute temperature, and K the equilibrium constant of the reaction.

Table 3. Lattice constants of quenched  $\text{YFeO}_3$

Sample	$-\log P_{\text{O}_2}/\text{atm}$	Time/h	Coexisting Phase	a/A	b/A	c/A	V/A <sup>3</sup>
Y <sub>2</sub> O <sub>3</sub> Fe <sub>2</sub> O <sub>3</sub>							
0.6 0.4	0.68	70	Y <sub>2</sub> O <sub>3</sub>	5.592(2)	7.609(4)	5.288(2)	225.0(2)
Ref. 15)				5.5946	7.6053	5.2817	

Four chemical reactions

were found in the established phase diagram, as

Table 4. The Gibbs Energy Change of Reactions at 1000°C

Reaction	$-\log(P_{\text{O}_2}/\text{atm})$	$-\Delta G^\circ/\text{kJmol}^{-1}$
1) Fe + 1/2 O <sub>2</sub> = FeO	15.22 (14.91) (14.94)	185.6 181.8* 182.1**
2) 3 FeO + 1/2 O <sub>2</sub> = Fe <sub>3</sub> O <sub>4</sub>	13.38 13.38 (13.56) (13.22)	165.5 168.8 <sup>a)</sup> 165.3* 161.2**
3) 2/3 Fe <sub>3</sub> O <sub>4</sub> + 1/6 O <sub>2</sub> = Fe <sub>2</sub> O <sub>3</sub>	6.02 (5.16) (5.33)	24.5 21.0* 21.7**
4) Fe + 1/2 Y <sub>2</sub> O <sub>3</sub> + 3/4 O <sub>2</sub> = YFeO <sub>3</sub>	15.41 (15.07) (15.15)	281.8 275.7*** 277.1****

\* These values were calculated from the Gibbs energy data of JANAF Table (4).

\*\* These values were calculated from the data of Ref. 16

\*\*\* This value was calculated by combining the value of Ref. 10 and the value of the formation of NiO in Ref. 16.

\*\*\*\* This value was calculated based on the data of 1/2 Fe<sub>2</sub>O<sub>3</sub> + 1/2 Y<sub>2</sub>O<sub>3</sub> = YFeO<sub>3</sub> (Ref. 17) and the value of the reaction Fe + 3/4 O<sub>2</sub> = 1/2 Fe<sub>2</sub>O<sub>3</sub>, which was calculated based on JANAF Table (4).

a) This value was calculated based on the activity of FeO(W<sub>2</sub>) in Table 2.

represented in Table 4. In calculation of the Gibbs energy changes of reactions the activity of each component has to be used. For example, as is apparent from the phase diagram, the activity of FeO in reaction 1) is different from that of reaction 2). That is, the activity of the FeO component at the composition W<sub>1</sub> in Fig. 1b, which is in equilibrium with Fe should be different from that of FeO at the composition W<sub>2</sub>,

which is in equilibrium with  $\text{Fe}_3\text{O}_4$ .

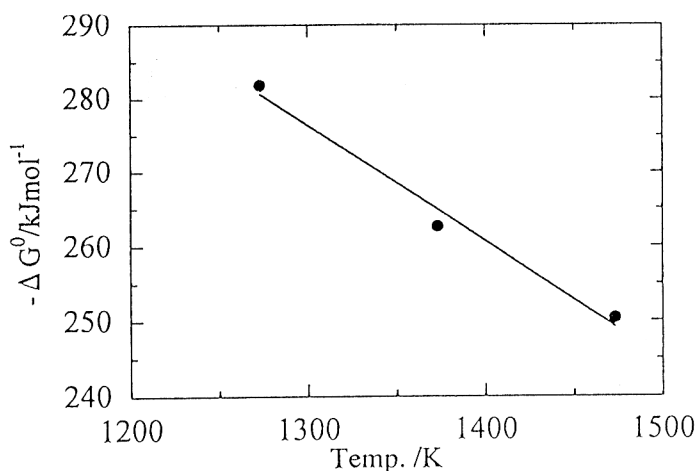


Fig. 4 The relationship between  $\Delta G^0$  for reaction 4) and the temperature.

The Gibbs-Duhem equation was used to calculate the activities of Fe and FeO components in the FeO solid solution from the obtained  $N_{\text{O}}/N_{\text{Fe}}$  relation. The details of the calculation can be found in the report of Darken and Gurry (1), and in the book by Wagner (14). In Table 4, values obtained in the present experimental conditions are shown. The values of  $\log(P_{\text{O}_2}/\text{atm})$  in parentheses were cal-

culated from the corresponding  $\Delta G^0$  values.

The  $\Delta G^0$  value of  $-185.6 \text{ kJmol}^{-1}$  for reaction 1) determined in the present investigation agrees well with the values  $-181.8$  and  $-182.1 \text{ kJmol}^{-1}$  calculated from the values of JANAF (4) and those of Robie et al.(16), respectively. Also, values for reactions 2) and 3), in the present study are in fairly good agreement with those calculated from JANAF (4) and (16).

The value  $-275.7 \text{ kJmol}^{-1}$  for the reaction 4) was calculated by combining the value of a reaction,  $\text{Fe} + 3/2 \text{ NiO} + 1/2 \text{ Y}_2\text{O}_3 = 3/2 \text{ Ni} + \text{YFeO}_3$ , of Yamauchi et al. (10), and the value of the formation of NiO with the value compiled by Robie et al. (16). Also, the value  $-277.1 \text{ kJmol}^{-1}$  for the reaction 4) was calculated based on the data (17) of the reaction  $1/2 \text{ Fe}_2\text{O}_3 + 1/2 \text{ Y}_2\text{O}_3 = \text{YFeO}_3$ , and the value of the reaction  $\text{Fe} + 3/4 \text{ O}_2 = 1/2 \text{ Fe}_2\text{O}_3$ , which was calculated based on JANAF Table (4).

The Present  $\Delta G^0$  value for reaction 4) is in fairly good agreement with the above previous values.

In Fig. 4, the relationship between the  $\Delta G^0$  for the reaction 4) and the temperature is shown. Values obtained at  $1100^\circ\text{C}$  and  $1200^\circ\text{C}$  were quoted from 18) and 5), respectively. A reasonable linear equation,  $\Delta G^0 = -4.811 \times 10^2 + 1.575 \times 10^{-1}T$ , was obtained by means of the least-squares method.

#### 4. Conclusion

- (1) Phase equilibrium in the Y-Fe-O system at  $1000^\circ\text{C}$  was established under an oxygen partial pressure from 0 to  $-16.15$  in  $\log(P_{\text{O}_2}/\text{atm})$ .
- (2) Under the present experimental conditions,  $\text{Y}_2\text{O}_3$ , Fe, "FeO",  $\text{Fe}_3\text{O}_4$ ,  $\text{Fe}_2\text{O}_3$ , and

YFeO<sub>3</sub> phases were stable, whereas YFe<sub>2</sub>O<sub>4</sub> and Y<sub>3</sub>Fe<sub>5</sub>O<sub>12</sub>(YIG) were not stable. This is a striking contrast to the previous results obtained at 1100°C and 1200°C.

- (3) Fe<sub>3</sub>O<sub>4</sub> and YFeO<sub>3</sub> were nonstoichiometric, but the range of the nonstoichiometry of Fe<sub>3</sub>O<sub>4</sub> was too small to be seen in Fig. 1a, b, and Fig. 3.
- (4) The lattice constants of YFeO<sub>3</sub> were determined and compared with previous values. The values obtained are comparable to the previous values.
- (5) The Gibbs energies changes of reactions found in the phase diagram were calculated with the oxygen partial pressures in equilibrium with three solid phases.
- (6) The relationship between  $\Delta G^0$  and the temperature for reaction 4) was obtained.

#### Reference

- 1) L. S. Darken and R. W. Gurry, J. Am. Chem. Soc., 67, (1945) 1398.
- 2) L. S. Darken and R. W. Gurry, J. Am. Chem. Soc., 68, (1946) 798.
- 3) A. Muan and E. F. Osborn, Phase equilibria among oxides in steelmaking, Addison-Wesley Publishing Company, Inc. 1965.
- 4) JANAF Thermochemical Tables, 2nd Ed., NSRDS-NBS 37, 1971.
- 5) N. Kimizuka and T. Katsura, J. Solid State Chem., 13, (1975) 176.
- 6) W. Piekarczyk, W. Weppner, and A. Rabenau, Mater. Sci. Monogr., 10, (1982) 679.
- 7) K. Kato, I. Kawada, N. Kimizuka, and T. Katsura, Z. Krist., 141, (1975) 314.
- 8) T. Matsumoto, N. Mori, J. Iida, M. Tanaka, K. Siratori, F. Izumi, and H. Asano, Physica B 180&181, (1992) 603.
- 9) G. G. Charette and S. N. Flengas, J. Electrochem. Soc., 115, (1968) 796.
- 10) S. Yamauchi, K. Fueki, T. Mukaibo, and C. Nakayama, Bull. Chem. Soc. Jpn., 48, (1975) 1039.
- 11) K. Kitayama, K. Nojiri, T. Sugihara, and T. Katsura, J. Solid State Chem., 56, (1985) 1.
- 12) T. Katsura and H. Hasegawa, Bull. Chem. Soc. Jpn., 40, (1967) 561.
- 13) K. Kitayama, J. Solid State Chem., 137, (1998) 255.
- 14) C. Wagner, Thermodynamics of Alloys, Addison-Wesley Publishing Company, Inc. 1952.
- 15) JCPDS Card No. 39-1489
- 16) R. A. Robie, R. S. Hemingway, and J. R. Fisher, Thermodynamic Properties of Minerals and Related Substances at 298.15 K and 1 Bar (10<sup>5</sup> Pascals) Pressure and at Higher Temperatures, Geological Survey Bulletin 1452. United States

Government Printing Office, Washington: 1978

- 17) Yu. Ya. Skolis, S. V. Kitsenko, and V. A. Levitskii, Zh. Fiz. Khim., 59, (1985) 2356 .
- 18) K. Kitayama, M. Sakaguchi, Y. Takahara, H. Endo, and H. Ueki, J. Solid State Chem., 177 (2004) 1933.